

First report and integrated analysis of two native *Trissolcus* species utilizing *Bagrada hilaris* eggs in California

Fatemeh Ganjisaffar¹, Elijah J. Talamas², Marie Claude Bon³, Thomas M. Perring¹

1 Department of Entomology, University of California, Riverside CA 92521, USA **2** Florida State Collection of Arthropods, Division of Plant Industry, Florida Department of Agriculture and Consumer Services, Gainesville, FL 32608, USA **3** USDA-ARS European Biological Control Laboratory, 810 Avenue du Campus Agropolis, 34980 Montferrier le Lez, France

Corresponding author: Elijah J. Talamas (billy.jenkins@gmail.com)

Academic editor: Petr Jansta | Received 28 July 2020 | Accepted 18 November 2020 | Published 29 December 2020

<http://zoobank.org/6DE3A894-CDFC-4D3C-946E-25E492C4C851>

Citation: Ganjisaffar F, Talamas EJ, Bon MC, Perring TM (2020) First report and integrated analysis of two native *Trissolcus* species utilizing *Bagrada hilaris* eggs in California. Journal of Hymenoptera Research 80: 49–70. <https://doi.org/10.3897/jhr.80.57024>

Abstract

Surveys with sentinel eggs of *Bagrada hilaris* (Hemiptera: Pentatomidae) in southern California retrieved two parasitoids that were not previously known to be associated with this stink bug, *Trissolcus hollensis* and *T. utahensis* (Hymenoptera: Scelionidae). Molecular and morphological analysis of these specimens is used to modify the concept of *T. utahensis* and assess the factors that contribute to intraspecific variation. We provide an updated couplet to separate *T. utahensis* from a morphologically similar species, *T. cosmopeplae*.

Keywords

Bagrada bug, egg parasitoids, painted bug, Scelionidae, sentinel eggs

Introduction

Bagrada hilaris (Burmeister) (Hemiptera: Pentatomidae) is native to Africa, Asia, and the Middle East (Howard 1907; Husain 1924). This stink bug first was reported in the United States in Los Angeles County, California, in 2008 (Arakelian 2008). By 2015, it had spread to 21 other counties in California, and six other states (Nevada, Arizona,

Utah, New Mexico, Texas, and Hawaii) (Palumbo and Natwick 2010; Palumbo et al. 2016; Bundy et al. 2012, Vitanza 2012; Perring et al. 2013; Reed et al. 2013; Matsunaga 2014). *Bagrada hilaris* also has been reported from six states of Mexico (Sánchez-Peña 2014; Torres-Acosta and Sánchez-Peña 2016; Hernández-Chávez et al. 2018) and Chile (Faúndez et al. 2016; Faúndez et al. 2017). *Bagrada hilaris* attacks various vegetable crops, weedy mustards, and several ornamental plants within the mustard family (Brassicaceae). In the United States, *B. hilaris* has been a serious pest of cole crops (Perring et al. 2013; Reed et al. 2013; Palumbo et al. 2016). The bugs are particularly damaging to young seedlings, but they also feed on leaves, stems, flowers, and seeds of older plants (Palumbo and Natwick 2010; Huang et al. 2014).

Chemical applications have been the main approach used against this pest (Palumbo 2015) and efforts to establish a biological control program were initiated in 2014. Three egg parasitoids of *B. hilaris* were collected in Pakistan (Mahmood et al. 2015) and brought to the United States to be evaluated as biological control candidates: *Trissolcus hyalinipennis* Rajmohana & Narendran (Rajmohana 2006), *Gryon gonikopalense* Sharma (Platygastroidea: Scelionidae) (Sharma 1982), and *Ooencyrtus mirus* Triapitsyn & Power (Chalcidoidea: Encyrtidae) (Triapitsyn et al. 2020). Laboratory evaluations of these parasitoids are still ongoing, and no release permits have been issued to date (Sforza et al. 2017; Martel et al. 2019; Power et al. 2020a, b). Meanwhile, monthly surveys using *B. hilaris* sentinel eggs have been conducted in California since the fall of 2017 to identify potential native or introduced parasitoids. Through these surveys, two scelionid species, *T. hyalinipennis* and *Trissolcus basalis* (Wollaston) (Ganjisaffar et al. 2018), and a new encyrtid species, *Ooencyrtus lucidus* Triapitsyn & Ganjisaffar (Triapitsyn et al. 2020), have been identified. This study reports the discovery and identification of two additional scelionid species that parasitized *B. hilaris* sentinel eggs in southern California: *Trissolcus hullensis* (Harrington) and *Trissolcus utahensis* (Ashmead).

Our analysis includes *T. utahensis* reared from sentinel eggs of *Podisus maculiventris* (Say) (Hemiptera: Pentatomidae) in British Columbia, Canada, to assess the limits of this species and determine its intraspecific variation using molecular and morphological data. Previous identification of the Canadian specimens brought attention to problems with the couplet that separates *T. utahensis* and *Trissolcus cosmopeplae* (Gahan) in the key to Nearctic *Trissolcus* of Talamas et al. (2015). This key has been used in annual workshops to identify stink bug egg parasitoids throughout North America, during which this couplet has proven to be problematic as well. We here employ molecular phylogenetics to determine which characters are variable, and which are sufficiently stable to be used for identification in these species, and we provide an updated couplet for *T. utahensis* and *T. cosmopeplae*.

Materials and methods

Survey locations

The Agricultural Operations of the University of California, Riverside, was the main site for the surveys. Fields that had been planted for various research were used for



Figure 1. Survey locations are displayed in red dots. The black rectangle shows the Agricultural Operations of the University of California, Riverside, where most of our surveys were conducted. Five *Trissolcus hullensis* were recovered from an alfalfa field (33.96508°N , $117.34084^{\circ}\text{W}$), one *Trissolcus utahensis* was recovered from a squash field with mustard weeds (33.96611°N , $117.34230^{\circ}\text{W}$), and eleven *T. utahensis* were recovered from roadside mustard weeds (33.99105°N , $117.33360^{\circ}\text{W}$).

our sentinel egg deployments. A mixed vegetable field available from October 2017 to March 2018, an alfalfa field (*Medicago sativa* L.) available from October 2017 to January 2019, and a squash field (*Cucurbita moschata* L., variety black futsu) available from January 2018 to September 2019 were used. The mixed vegetable field was selected particularly because of its two rows of broccoli (*Brassica oleracea* L., variety Italica), a favorable host for *B. hilaris*. The alfalfa field hosted several stink bug species during spring and summer, serving as a potential source of stink bug egg parasitoids. The squash field was selected because *B. hilaris* adults were found on shortpod mustard weeds, *Hirschfeldia incana* (L.) Lagr.-Foss., within the field. Surveys also were conducted at other locations on the Agricultural Operations property where mustard weeds were found. In addition, various locations in the urban area with brassicaceous weeds surrounding the University of California, Riverside, were surveyed (Fig. 1). Previous monthly samplings from January to December 2011 by Reed et al. (2013) had shown that the primary weeds supporting *B. hilaris* in this area were London rocket (*Sisymbrium irio* L.), shepherd's purse (*Capsella bursa-pastoris* (L.) Medik.), and shortpod mustard. *Bagrada hilaris* also were found occasionally on Russian thistle (*Salsola australis* R.Br.) and telegraph weed (*Heterotheca grandiflora* Nutt.) when they were in close proximity to senesced shortpod

mustard. According to Reed et al. (2013), these weeds were available following fall and winter rains through June and the peak *B. hilaris* abundance was during the spring on these host plants. We used the same locations for our sentinel egg deployments, and surveys were conducted monthly from 21 October 2017 through 27 September 2019.

Sentinel egg card preparation and parasitoid recovery

Bagrada hilaris eggs (≤ 24 hours old) were used for the surveys. Adult mating pairs of greenhouse-grown *B. hilaris* (Reed et al. 2017) were maintained on organic broccoli florets in plastic containers (15 cm diameter \times 6.5 cm height) with 2 screen openings for air circulation in an insectary room at 30 ± 1 °C, 40–50% humidity and 14:10 (L:D) photoperiod. White paper towels were cut in circles to fit the bottom of each container to provide a substrate for oviposition. Approximately 15 mating pairs were placed into each container. *Bagrada hilaris* eggs were collected daily and glued (Gorilla Super Glue Gel, The Gorilla Glue Co., Ohio, USA) on a 3×5 grid of squares on a weatherproof card so that each card contained 15 eggs (Ganjisaffar et al. 2018). For each location, a sentinel card was taped to the wire of a landscape flag, positioning it about 30 cm from the ground. Previous studies showed that eggs placed on cards on the soil surface were eaten by predators (Ganjisaffar et al. 2018). The number of cards used for each survey date varied from 10 to 20, depending on the availability of *B. hilaris* eggs. Cards were left in the field for 3–5 days (3.7 days on average) to avoid *B. hilaris* eggs from hatching in the field. According to Reed et al. (2017), *B. hilaris* eggs hatch after 5 days at temperatures approximating the warmest temperatures on the days of the field surveys. Once collected, the grid was cut and placed in glass vials plugged with cotton. The vials were maintained in the same insectary room that was used for the *B. hilaris* colony and were examined for parasitism and wasp emergence. Emerged wasps were transferred to vials containing 95% ethanol for identification.

Molecular analysis

Genomic DNA was non-destructively isolated from the entire specimen using the Qia- gen DNeasy Blood and Tissue kit (Hilden, Germany) as described in Sabbatini Peverieri et al. (2018). A comprehensive list of all samples extracted with author and year, host, and locality data is given in Table 1 in Supporting Information. The barcode region of the mitochondrial Cytochrome Oxidase Subunit I (*COI*) was amplified using the universal barcoding primer set LCO1490/HCO2198 (Folmer et al. 1994) (Table 1). The primer set LCO1490puc (Craaud et al. 2009)/C1-N-2353 (Simon et al. 2006) was used in six samples to amplify a longer region (~850 bp) than the classical barcode region (~710 bp), providing more than enough coverage for the barcode that is not always obtained when using universal primer sets (Table 1). All PCRs were performed as described in Ganjisaffar et al. (2018), except the PCR conditions. The thermocycling conditions were as follows: 1 cycle of denaturation at 94 °C for 3 min, 35 cycles at 94 °C for 30 s, 52 °C (LCO1490/HCO2198) or 50 °C (LCO1490puc/C1-N-2353) for 30 s, 72 °C for 1 min with a final extension step of 10 min at 72 °C. All samples were

Table I. Collection data on samples of *Trissolcus utahensis*, *T. bullensis* and *T. colemani* obtained in this study, and corresponding *COI* information.

Sample ID	Collection Unit	Species (Hymenoptera: Scelionidae)	Host (Hemiptera: Pentatomidae)	Location	Date collected; name of the collector	Primers for mt-CO1 PCR and sequencing	DNA depository	COI Genbank Accession number
TSP274	FSCA 00000302	<i>Trissolcus utahensis</i>	<i>Podisus maculiventris</i>	Penticton, BC, Canada	July 2017; W. Wong & Paul Abram	LCO1490/HCO2198	EBCL	MT804738
TSP276	FSCA 00033040	<i>Trissolcus utahensis</i>	<i>Podisus maculiventris</i>	Penticton, BC, Canada	June 2017; W. Wong & Paul Abram	LCO1490/HCO2198	EBCL	MT804739
TSP277	FSCA 00033041	<i>Trissolcus utahensis</i>	<i>Podisus maculiventris</i>	Penticton, BC, Canada	June 2017; W. Wong & Paul Abram	LCO1490/HCO2198	EBCL	MT804740
TSP278	FSCA 00033042	<i>Trissolcus utahensis</i>	<i>Podisus maculiventris</i>	Penticton, BC, Canada	August 2017; W. Wong & Paul Abram	LCO1490/HCO2198	EBCL	MT804741
TSP279	FSCA 00033043	<i>Trissolcus utahensis</i>	<i>Podisus maculiventris</i>	Penticton, BC, Canada	August 2017; W. Wong & Paul Abram	LCO1490/HCO2198	EBCL	MT804742
TSP280	FSCA 00033044	<i>Trissolcus utahensis</i>	<i>Podisus maculiventris</i>	Penticton, BC, Canada	June 2017; W. Wong & Paul Abram	LCO1490/HCO2198	EBCL	MT804743
TSP281	FSCA 00033045	<i>Trissolcus utahensis</i>	<i>Podisus maculiventris</i>	Penticton, BC, Canada	June 2017; W. Wong & Paul Abram	LCO1490/HCO2198	EBCL	MT804744
TSP288	FSCA 00033239	<i>Trissolcus utahensis</i>	<i>Bagrada hilaris</i>	Riverside California, USA	October 2018; Fatemeh Ganjiaffar	LCO1490/HCO2198	EBCL	MT804745
PL141	FSCA 00091859	<i>Trissolcus utahensis</i>	<i>Bagrada hilaris</i>	Riverside California, USA	October 2018; Fatemeh Ganjiaffar	LCO1490/HCO2198	FSCA	MT804746
PL142	FSCA 00091872	<i>Trissolcus utahensis</i>	<i>Bagrada hilaris</i>	Riverside California, USA	October 2018; Fatemeh Ganjiaffar	LCO1490/HCO2198	FSCA	MT804747
PL259	FSCA 00094712	<i>Trissolcus utahensis</i>	<i>Podisus maculiventris</i>	Penticton, BC, Canada	July 2017; W. Wong & Paul Abram	LCO1490/HCO2198	FSCA	MT804748
PL260	FSCA 00094711	<i>Trissolcus utahensis</i>	<i>Podisus maculiventris</i>	Penticton, BC, Canada	May 2017; W. Wong & Paul Abram	LCO1490/HCO2198	FSCA	MT804749
PL261	FSCA 00094713	<i>Trissolcus utahensis</i>	<i>Podisus maculiventris</i>	Penticton, BC, Canada	August 2017; W. Wong & Paul Abram	LCO1490/HCO2198	FSCA	MT804750
PL262	FSCA 00094714	<i>Trissolcus utahensis</i>	<i>Podisus maculiventris</i>	Penticton, BC, Canada	August 2017; W. Wong & Paul Abram	LCO1490/HCO2198	FSCA	MT804751
PL263	FSCA 00094715	<i>Trissolcus utahensis</i>	<i>Podisus maculiventris</i>	Penticton, BC, Canada	August 2017; W. Wong & Paul Abram	LCO1490/HCO2198	FSCA	MT804752
TSP291	FSCA 00090585	<i>Trissolcus bullensis</i>	<i>Halymorpha halys</i>	St. Helena, CA, USA	August 2017; Kent Daane	LCO1490/HCO2198	EBCL	MT804753
PL143	FSCA 00091873	<i>Trissolcus bullensis</i>	<i>Bagrada hilaris</i>	Riverside, CA, USA	March 2019; Fatemeh Ganjiaffar	LCO1490/HCO2198	FSCA	MT804754
PL144	FSCA 00091874	<i>Trissolcus bullensis</i>	<i>Bagrada hilaris</i>	Riverside, CA, USA	March 2019; Fatemeh Ganjiaffar	LCO1490/HCO2198	FSCA	MT804755
TSP398	FSCA 00094753	<i>Trissolcus colemani</i>	<i>Piesodorus lituratus</i>	Assas, France	June 2011; Marie Roche	LCO-1490puc/C1-N-2353	EBCL	MT804756
TSP400	FSCA 00094754	<i>Trissolcus colemani</i>	<i>Eurydema ventralis</i>	Montferrier le Lez, France	May 2019; Marie Roche	LCO-1490puc/C1-N-2353	EBCL	MT804757
TSP401	FSCA 00094755	<i>Trissolcus colemani</i>	<i>Eurydema ventralis</i>	Montferrier le Lez, France	May 2019; Marie Roche	LCO-1490puc/C1-N-2353	EBCL	MT804758
TSP403	FSCA 00094756	<i>Trissolcus colemani</i>	<i>Dolycoris baccarum</i> (Hemiptera: Pentatomidae)	Montferrier le Lez, France	July 2010; Marie Roche	LCO-1490puc/C1-N-2353	EBCL	MT804759
TSP409	FSCA 00094757	<i>Trissolcus colemani</i>	<i>Graphosoma italicum</i>	Montferrier le lez, France	July 2019; Marie Roche	LCO-1490puc/C1-N-2353	EBCL	MT804760
TSP410	FSCA 00094758	<i>Trissolcus colemani</i>	<i>Graphosoma italicum</i>	Montferrier le lez, France	July 2019; Marie Roche	LCO-1490puc/C1-N-2353	EBCL	MT804761

sequenced bidirectionally using the BigDye chemistry by Genoscreen (Lille, France) or the ABI SeqStudio Platform at FDACS-DPI in Florida (USA). A *COI* consensus sequence was established for each specimen. All sequences generated from this study are deposited in GenBank, and all residual DNAs are archived at EBCL or FSCA (Table 1).

Voucher specimens which have been reexamined following the molecular analysis are presently archived at FSCA (Table 1). All sequences were translated into amino acids to check for stop codons and frame shifts. All sequences obtained were compared with sequences present in GenBank using the Basic Local Alignment Search Tool (<http://www.ncbi.nlm.nih.gov/BLASTn>). BOLD identification engine (Ratnasingham and Herbert 2007) was similarly datamined for barcodes of *Trissolcus* species and evaluated for barcode identification success. The 28 sequences obtained in this study were aligned with 28 barcode sequences of *Trissolcus* retrieved from GenBank. The final alignment of 56 sequences was performed using the default settings of CLUSTAL W (Thompson et al. 1994) as implemented in MEGA X (Kumar et al. 2018) and resulted in 576 characters with 174 parsimony informative sites. The phylogenetic relationships among specimens were reconstructed following a Bayesian analysis as implemented in MrBayes v. 3.2 (Ronquist et al. 2012). Searches were run for 1 million generations, in two independent runs, using default priors and the GTR+I+G substitution model that was selected using the Bayesian information criterion (BIC) in MEGA X. One sequence of *Trissolcus thyantae* Ashmead (GenBank MN615574.1) was specified as the outgroup based on the results of Talamas et al. (2019). Because a network approach is well adapted to infer intraspecific genealogical relationships, a haplotype network was built for *T. utahensis* using TCS 1.21 (Clement et al. 2000). As the resulting clades were not connected under 90% statistical parsimony limits, we reran the TCS analysis by fixing connection limits at 50 steps. To estimate the divergence within and between terminal taxa and clades, we calculated the uncorrected p-distance using MEGA X, since the generally used K2P distance (Kimura 1980) could be inappropriate when applied to closely related taxa (Srivathsan and Meier 2012).

Morphology

Terminology follows that of Talamas et al. (2017). Following non-destructive DNA extraction, six specimens used in the molecular analysis were photographed (1 *T. hullensis* and 7 *T. utahensis*) to document morphology of specimens from different haplogroups and those reared from different hosts. Images were produced with a Macropod imaging system. Image stacks were rendered with Helicon Focus and further processed in Adobe Photoshop CS6.

Abbreviations and characters annotated in the figures

aem anteroventral extension of the metapleuron (Figs 6, 13)
gc genal carina (Fig. 16)
msct metascutellum (Figs 4–5)
mshs mesoscutal humeral sulcus (Figs 6, 21)
mtnm metanotum (Figs 4–5)

mtpm metapostnotum (Figs 4–5)
not notaulus (Figs 7, 20, 22)
oc occipital carina (Figs 22, 25)
ppm propodeum (Figs 4–5)

Results

Field surveys

Our survey period of March 6–9, 2018, in the alfalfa field, yielded a sentinel card with 6 parasitized eggs from which 5 specimens of *T. hullensis* and 1 specimen of *T. basalis* wasps emerged. A month later during our April 6–9, 2018, survey in the roadside mustard weeds (33.99105N, 117.33360W), two sentinel cards were parasitized; one of them had 5, and the other one had 7 parasitized eggs, which yielded 11 *T. utahensis*. One *T. utahensis* wasp was recovered from a sentinel card that was deployed in the squash field with mustard weeds on October 12–16, 2018.

Molecular analysis

The phylogenetic analysis based on the *COI* barcode data revealed a relatively well-resolved and supported topology identifying six terminal taxa (Fig. 2). The deepest node corresponds to the split between *T. utahensis* and the other species, including *T. hullensis*. The *T. hullensis* clade comprised two specimens reared from *B. hilaris* eggs and one specimen reared from frozen sentinel eggs of *Halyomorpha halys* (Stål) (Hemiptera: Pentatomidae) in Napa County, California. The *T. utahensis* cluster contains four main clades. The TCS analysis yielded four haplotype sub-networks, which were not connected under the 90% statistical parsimony limits, corresponding to these four clades of which clade 2 and clade 3 are each represented by a single haplotype, and clade 1 and clade 4 by three haplotypes each (Fig. 3). Clades 1, 3 and 4 contained specimens from British Columbia that were reared from *P. maculiventris* eggs. Clade 1 contained specimens from Canada and southern California, reared from the eggs of *P. maculiventris* and *B. hilaris*, respectively, indicating that they are conspecific. Interestingly, clade 2 included only Californian specimens reared from *B. hilaris*. Genetic distance between all clades ranged from 2.8% (clade 1/clade 2) to 9.9% (clade 1/clade 4) but remained lower than the range (from 10.6% to 14.3%) of interspecific distances obtained with the five other species in our analysis (Table 2).

Trissolcus hullensis (Harrington)

Remarks. The identification of *Trissolcus hullensis* is straightforward using the characters presented in Johnson (1985) and repeated in Talamas et al. (2015). Characters of the posterior mesosoma are particularly useful for determining this species: In

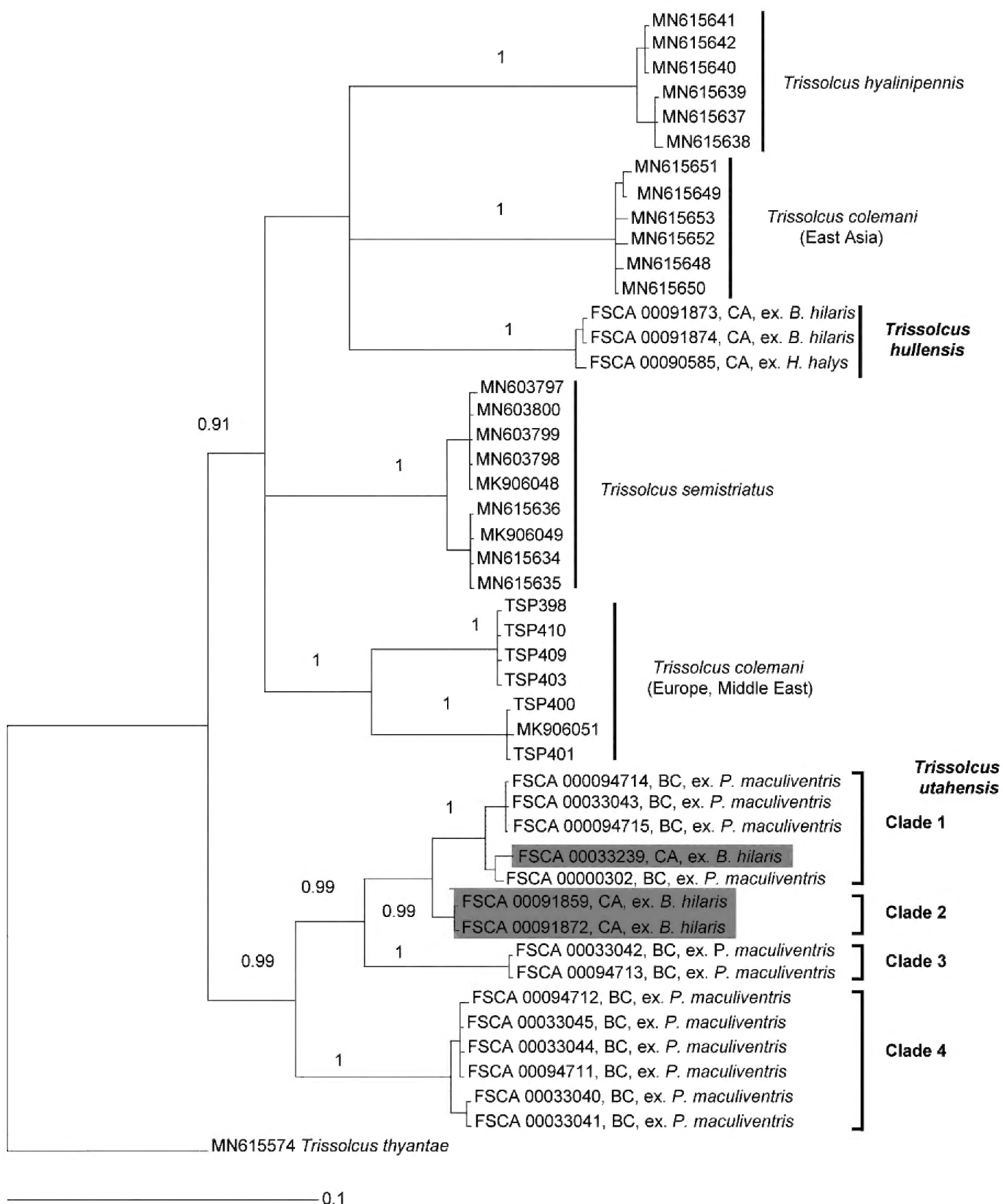


Figure 2. The Bayesian 50% majority rule consensus tree inferred from the 56 *COI* sequences of the six *Trissolcus* species including *T. hullensis* and *T. utahensis*. Only posterior probabilities >90% are indicated on the nodes. The tree is rooted with the outgroup *Trissolcus thyantae* (GenBank MN615574). The scale bar corresponds to 0.1 estimated substitutions per site.

T. hullensis the propodeum and metanotum are directly adjacent between the metapostnotum and metascutellum (Fig. 4), whereas in other species of Nearctic *Trissolcus*, the metapostnotum extends medially toward the metascutellum, and separates the propodeum from the metanotum (Fig. 5).

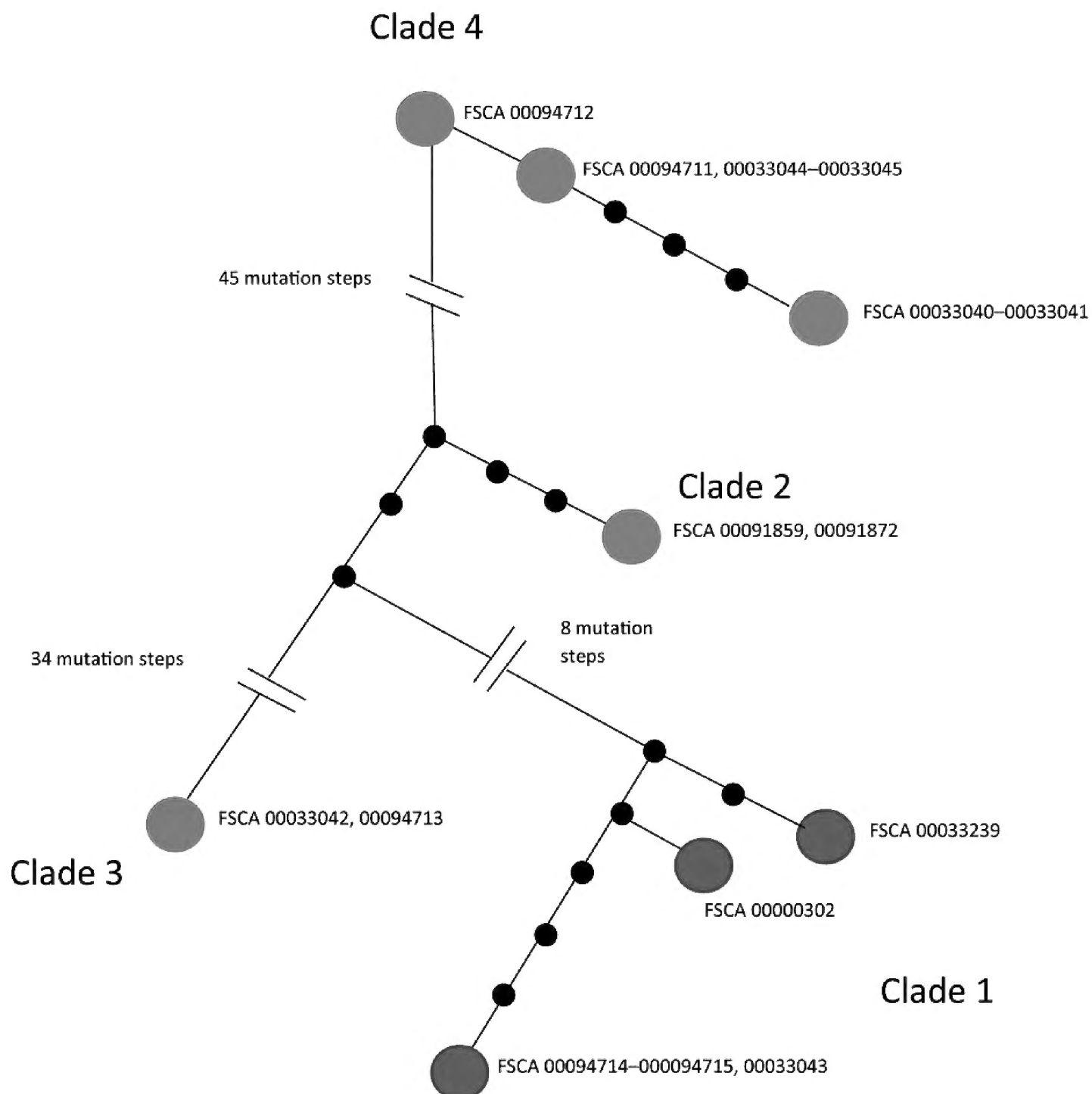


Figure 3. TCS *COI* haplotype network for the four clades of *T. utahensis* by fixing connection limits at 50 steps. Each haplotype is represented by a colored circle. Lines represent one mutational step between haplotypes, and dark circles represent unsampled haplotypes inferred from the data. Interrupted lines were used when haplotypes were separated by a long branch of more than 7 mutation steps.

Material Examined. 5 females, FSCA 00091873–00091874, 00091886–00091888 (deposited in FSCA) USA: CA: UC Riverside Agricultural Operations, 33.96508N, 117.34084W, alfalfa field, ex. *Bagrada hilaris* sentinel eggs deployed 6–9. III.2018, parasitoids emerged 23.III.2018, Coll. Ganjisaffar.

Trissolcus utahensis (Ashmead)

Remarks. The concept of *Trissolcus utahensis* was most recently treated in a revisionary context by Johnson (1985). This treatment separated *T. utahensis* from *T. cosmopeplae*

Table 2. Genetic distances (p-distances %, 1,000 bootstrap replications) for the *CO1* barcode at the levels of intra-species, inter-species and clades of *T. utahensis*. Data are expressed as mean ± S.E.

	<i>T. colemani</i> (East Asia)	<i>T. semistriatus</i>	<i>T. hyalinipennis</i>	<i>T. colemani</i> (Europe, Middle East)	<i>T. hullensis</i>	<i>T. utahensis</i> Clade 1	<i>T. utahensis</i> Clade 2	<i>T. utahensis</i> Clade 3	<i>T. utahensis</i> Clade 4
<i>T. colemani</i> (East Asia)	4.2 ± 0.6								
<i>T. semistriatus</i>	10.6 ± 1.18	0.7 ± 0.2							
<i>T. hyalinipennis</i>	13.3 ± 1.2	12.1 ± 1.3	0.4 ± 0.2						
<i>T. colemani</i> (Europe, Middle East)	12.7 ± 1.31	14.1 ± 1.4	14.3 ± 0.1	0.4 ± 0.1					
<i>T. hullensis</i>	12.5 ± 1.3	12.4 ± 1.3	13.1 ± 1.3	12.3 ± 1.4	0.2 ± 0.1				
<i>T. utahensis</i> Clade 1	11.4 ± 1.2	10.8 ± 1.3	14.2 ± 1.4	14.1 ± 1.4	13.1 ± 1.4	0.7 ± 0.2			
<i>T. utahensis</i> Clade 2	11.6 ± 1.2	10.8 ± 1.3	14.1 ± 1.4	14.3 ± 1.4	12.8 ± 1.3	2.8 ± 0.6	0		
<i>T. utahensis</i> Clade 3	12.6 ± 1.3	11.8 ± 1.3	16 ± 1.5	14.5 ± 1.4	12.2 ± 1.3	7.78 ± 1.1	7.12 ± 1.1	0	
<i>T. utahensis</i> Clade 4	11.9 ± 1.2	12.9 ± 1.3	12.6 ± 1.3	14.7 ± 1.5	11.9 ± 1.3	9.97 ± 1.1	8.65 ± 1.1	9.61 ± 1.2	0.4 ± 0.1

based on the length of the anteroventral extension of the metapleuron, the absence of a genal carina, the shape of the gena in lateral view, and if notaui could be distinguished from the surface sculpture of the posterior mesoscutum. These characters were used again in the key to Nearctic *Trissolcus* by Talamas et al. (2015), with the addition of the form of the mesoscutal humeral sulcus, which was treated as variable within *T. cosmopeplae*. Talamas et al. (2015) also treated the anteroventral extension of the metapleuron as variable within *T. cosmopeplae* and emphasized the shape of the gena in lateral view to separate these species. This modification to the key sought to reconcile variability in the shape of the gena with other, seemingly variable characters. The shape of the gena has proven to be one of the more difficult characters to interpret because there is not a discrete boundary between “narrow” and “bulging”. Because the variation in these characters does not correspond to clades in our phylogeny, we treat them as intraspecifically variable and the *T. utahensis* clade as a single species (Fig. 2). Based on the morphological analysis provided below we propose the following replacement for couplet 14 in Talamas et al. (2015):

14 Anteroventral extension of the metapleuron long, extending to base of mesocoxa (Fig. 6); mesoscutal humeral sulcus comprised of cells (Figs 6–7).....
..... *T. cosmopeplae* (Gahan)
– Anteroventral extension of the metapleuron short, not approaching base of mesocoxa (Figs 12–19); mesoscutal humeral sulcus indicated by a smooth furrow (Figs 20–22) *T. utahensis* (Ashmead)

Sculpture of the dorsal frons. Figs 8–11 illustrate variation in the size of the smooth area directly below the preocellar pit, and the striation that radiates from the

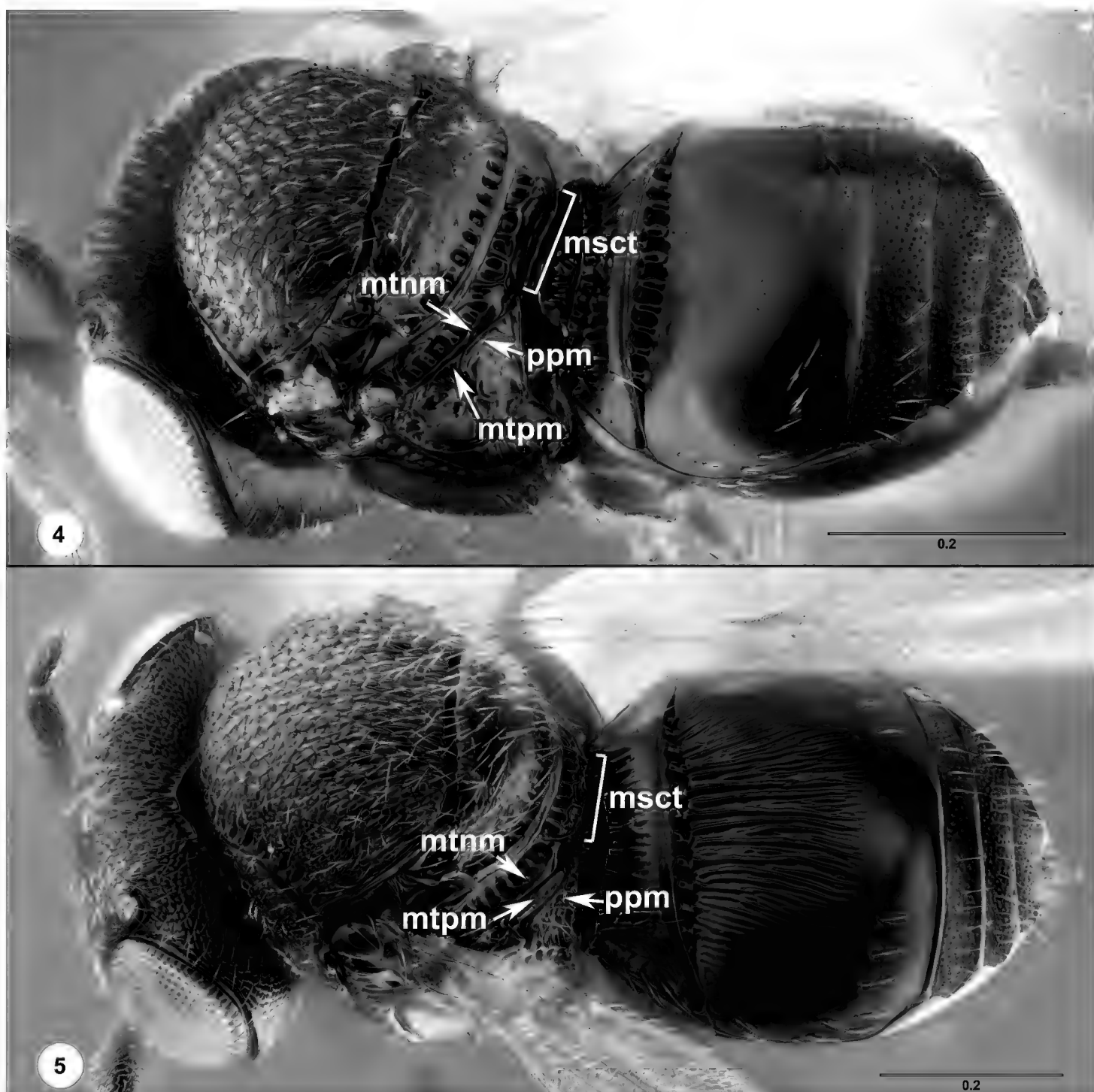
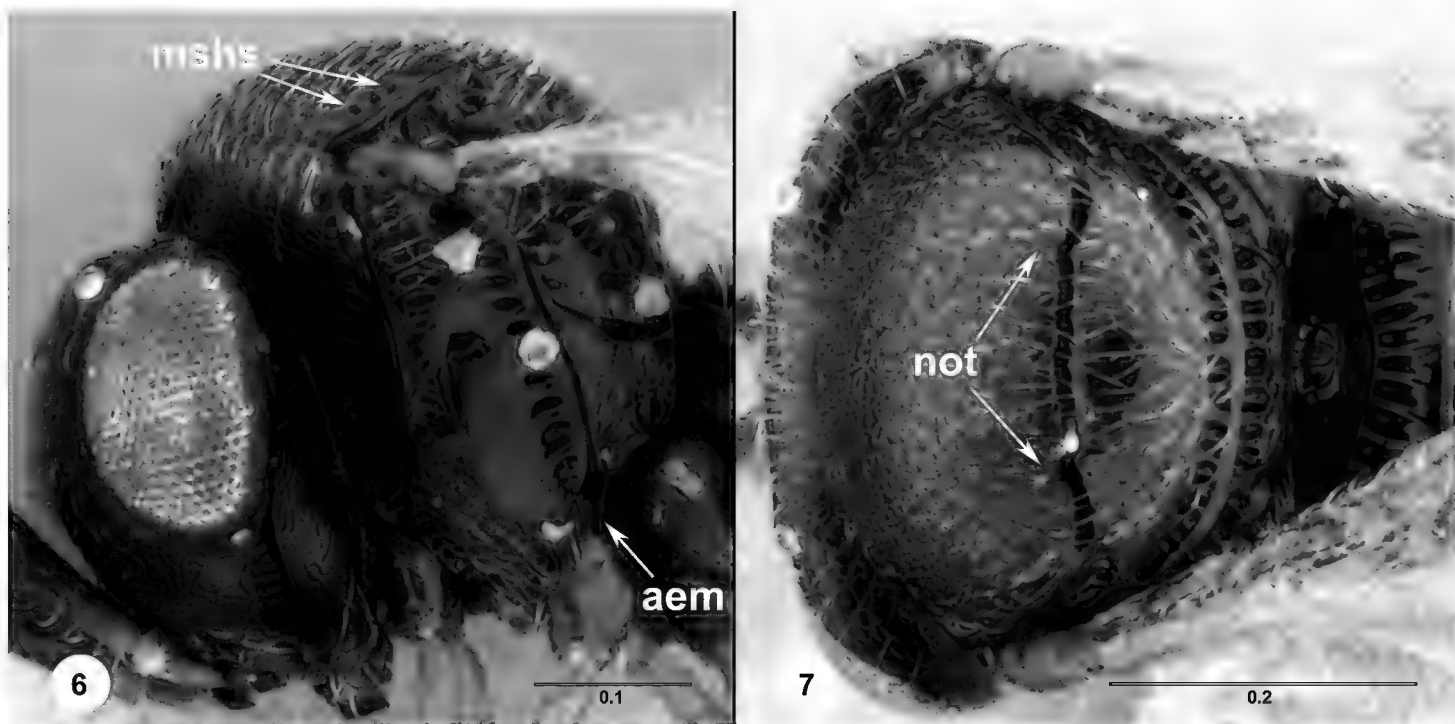


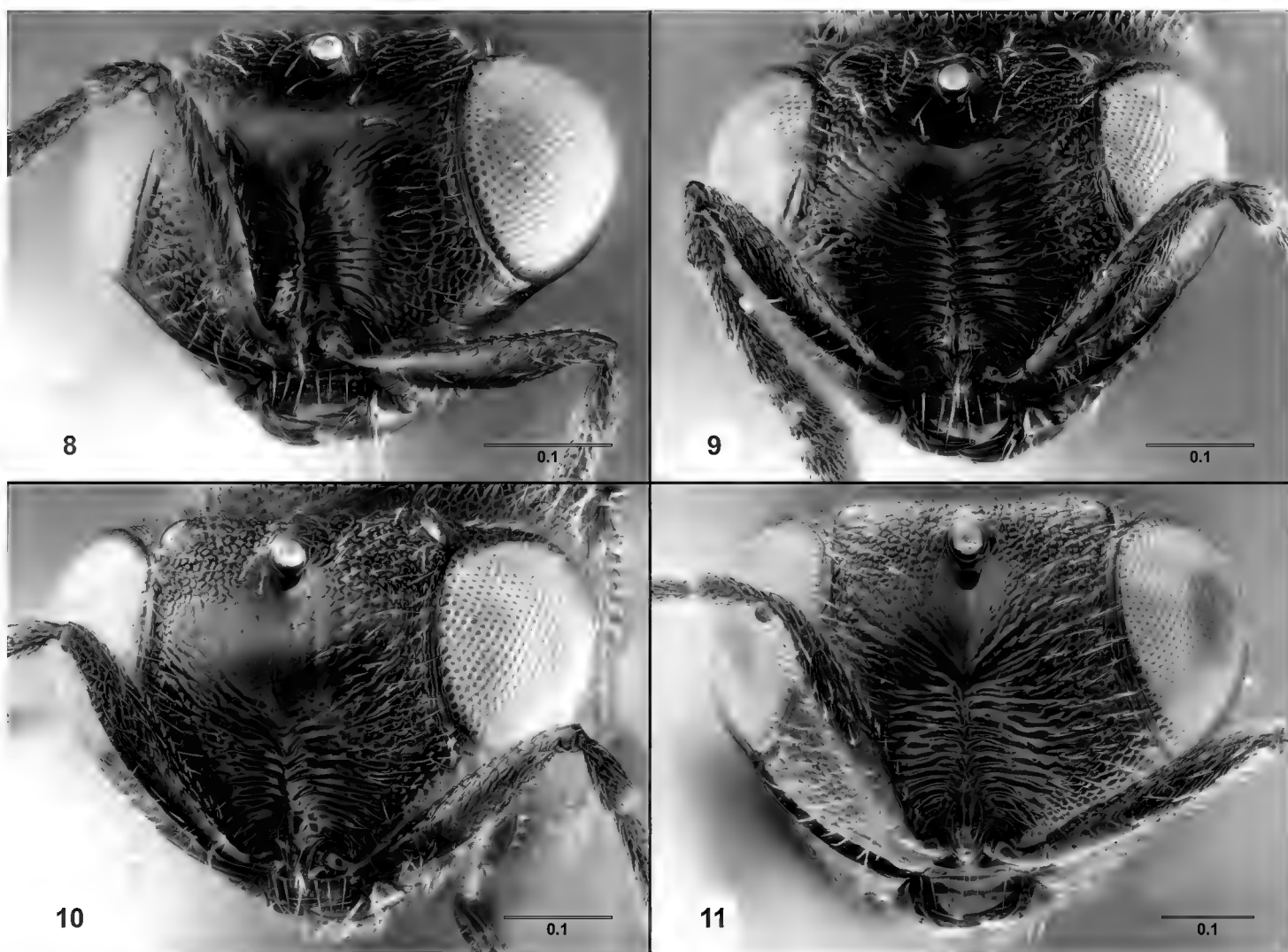
Figure 4–5. 4 *Trissolcus hullensis* (FSCA 00091886), head, mesosoma, metasoma, dorsolateral view
5 *T. utahensis* (FSCA 00000302), head, mesosoma, metasoma, dorsolateral view. Scale bars in millimeters.

antennal scrobe. Fig. 8 illustrates a specimen that emerged from a *B. hilaris* egg. As was found in *T. basalis*, specimens that developed in *B. hilaris* eggs have reduced sculpture relative to those that developed in other hosts (Ganjisaffar et al. 2018). The specimens in Figs 9, 11 were both reared from the eggs of *P. maculiventris* in British Columbia, and have identical COI barcode sequences, yet the size of smooth area on the dorsal frons differs between them. The specimen in Fig. 11 is the largest (1.35 mm) among these, and the specimen in Fig. 8 is the smallest (0.93 mm). The specimens in Figs 9, 10 have the smooth area on the frons about equal in size and these specimens are also approximately equal in length (1.11 and 1.07 mm, respectively). These two specimens were retrieved in different haplogroups (clades 1 and 4), and we thus postulate that sculptural differences on the frons are size dependent.

Variation on the gena. The shape of the gena varies between and within the four clades of *T. utahensis*. In clades 1 and 3, the specimens have a rather narrow gena, and

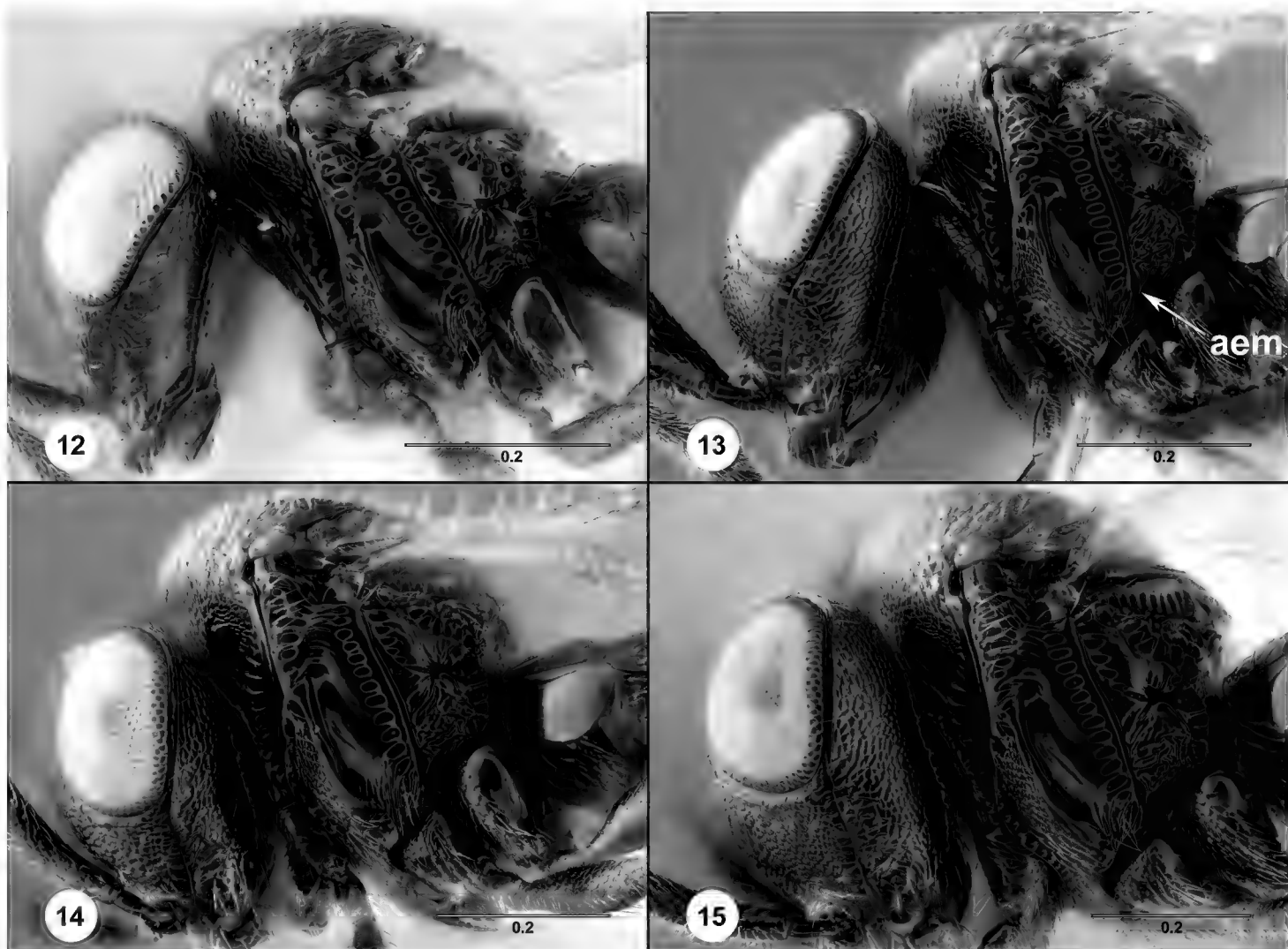


Figures 6–7. *Trissolcus cosmopeplae*, holotype female (USNMENT00989096) **6** head and mesosoma, lateral view **7** head and mesosoma, dorsal view. Scale bars in millimeters.



Figures 8–11. *Trissolcus utahensis*, head, anterior view **8** DPI_FSCA00033239 (ex. *B. hilaris*) **9** FSCA 00033041 (ex. *P. maculiventris*) **10** FSCA 00000302 (ex. *P. maculiventris*) **11** FSCA 00033040 (Ex. *P. maculiventris*). Scale bars in millimeters.

in clades 2 and 4 the gena is moderately to distinctly bulging in lateral view. Figs 12–15, 24 and 27 illustrate this variation. The degree to which the gena is bulging in lateral view does not appear to be host or size related. Specimens reared from *B. hilaris* eggs



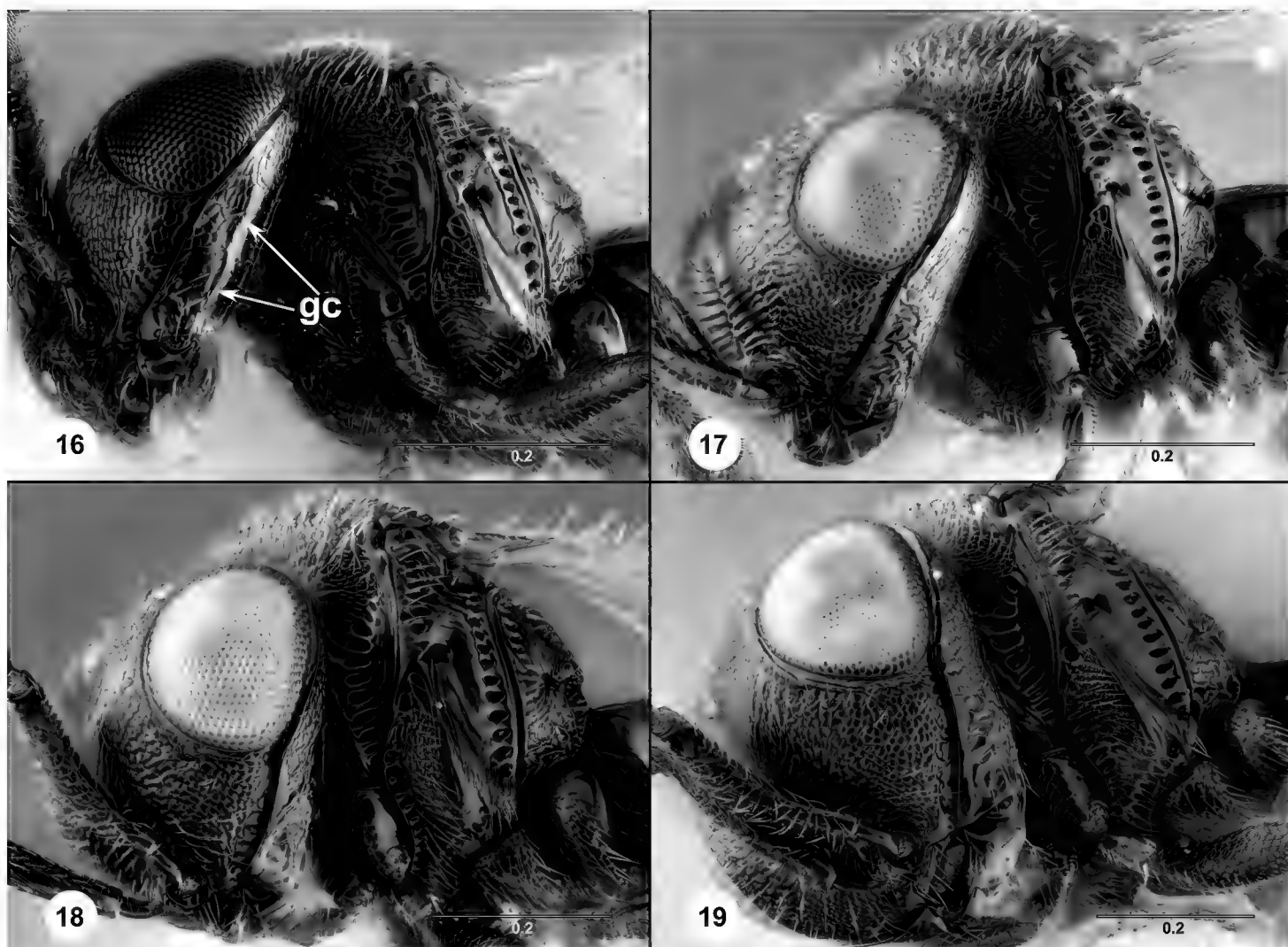
Figures 12–15. *Trissolcus utahensis*, head and mesosoma, lateral view **12** DPI_FSCA00033239 (ex. *B. hilaris*) **13** FSCA 00033041 (ex. *P. maculiventris*) **14** FSCA 00000302 (ex. *P. maculiventris*) **15** FSCA 00033040 (ex. *P. maculiventris*). Scale bars in millimeters.

are the smallest and have the gena moderately (Fig. 12) to distinctly (Fig. 24) bulging. The specimens with the most distinctly bulging gena (clade 4, Figs 15, 19) and the narrowest gena (clade 3, Figs 27, 28) were both reared from eggs of *P. maculiventris* and the specimens are larger than those reared from *B. hilaris* eggs.

Specimens with a bulging gena tend not to have the genal carina indicated, whereas specimens with a narrow gena often have it clearly expressed, but this is not an exact correlation. The specimen in Figs 12, 16 has a moderately bulging gena and the genal carina is distinctly present.

Microsculpture on the poster gena is less developed in specimens reared from *B. hilaris* eggs (Fig. 12), and this area is noticeably smoother than in specimens reared from *P. maculiventris* eggs (Figs 13–15). This phenomenon is consistent with a general pattern of reduced sculpture in smaller specimens.

Occipital carina. Tortorici et al. (2019) presented a new character to distinguish *T. semistriatus* (Nees von Esenbeck) from closely related species: the form of the occipital carina in dorsal view. In most species of *Trissolcus* the occipital carina is evenly convex, but in a few species, including *T. semistriatus* and *T. utahensis*, the occipital carina forms a distinct angle and the vertex of this angle may have a short carina directed toward the median ocellus (Figs 5, 22). In some specimens that emerged from *B. hilaris* eggs, the vertex of the angle formed by the occipital carina is less sharp, perhaps due to



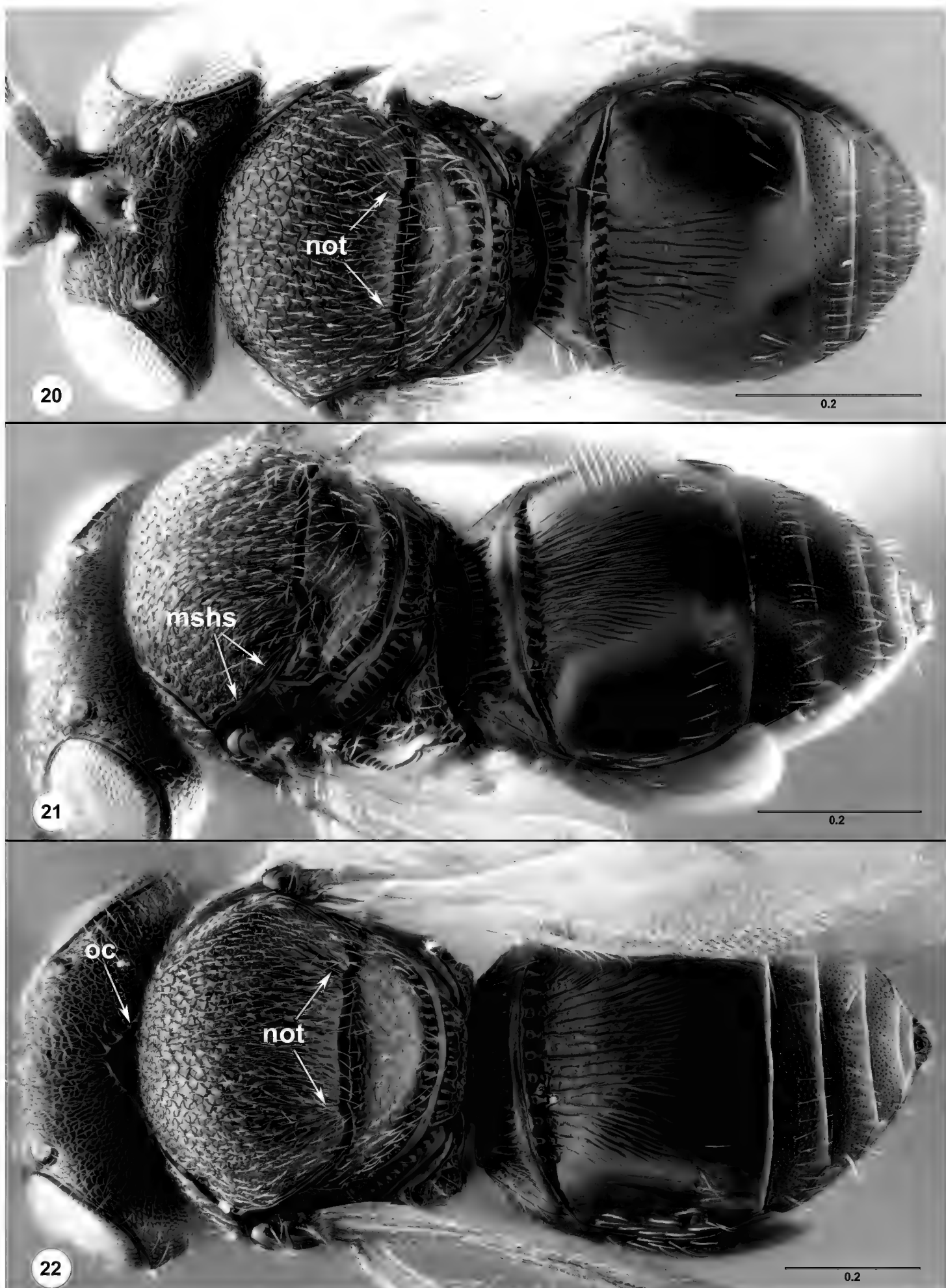
Figures 16–19. *Trissolcus utahensis*, head and mesosoma, ventrolateral view **16** DPI_FSCA00033239 (ex. *B. hilaris*) **17** FSCA 00033041 (ex. *P. maculiventris*) **18** FSCA 00000302 (ex. *P. maculiventris*) **19** FSCA 00033040 (e. *P. maculiventris*). Scale bars in millimeters.

its diminutive size (Fig. 25). The occipital carina is not visible in the available images of *T. cosmopeplae*, and it is obscured by glue in the holotype specimen of *T. utahensis*. This character deserves further attention in Nearctic *Trissolcus* although we are not presently able to determine if it can separate *T. cosmopeplae* and *T. utahensis*.

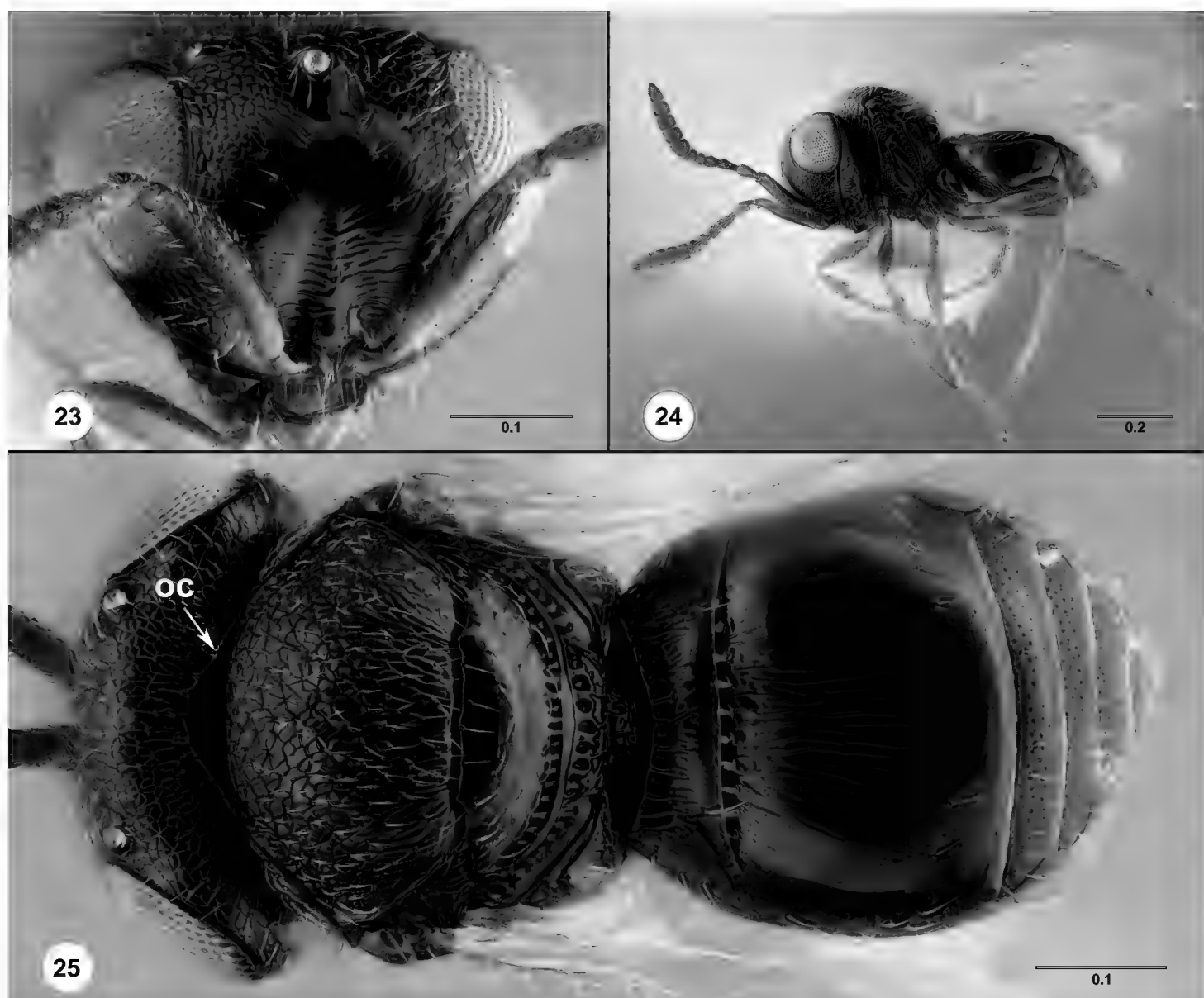
Notaulus. Specimens of *T. utahensis* reared from both *B. hilaris* and *P. maculiventris* have the notaulus indicated by short, shallow grooves present at the posterior margin of the mesoscutum (Figs 5, 20–22). These are visible in the holotype of *T. utahensis* (see fig. 100 in Talamas et al. (2015)), and they have the same form in the holotype of *T. cosmopeplae* (Fig. 7). Based on re-examination of images of the types and the specimens at hand, we conclude that this character does not separate these species.

Mesoscutal humeral sulcus. The form of the mesoscutal humeral sulcus was used by Tortorici et al. (2019) to separate very similar Palearctic *Trissolcus* species. This sulcus is clearly indicated by cells in the holotype of *T. cosmopeplae* (Figs 6, 7) and it is present as a smooth furrow in all specimens of *T. utahensis* that we have examined (Figs 5, 20–21), including the holotype.

Anteroventral extension of the metapleuron. The length of this structure, reaching to the mesocoxa in *T. cosmopeplae* (Fig. 6) and very short in *T. utahensis* (Figs 12–19),



Figures 20–22. *Trissolcus utahensis* **20** FSCA 00033239 (ex. *B. hilaris*), head, mesosoma, metasoma, dorsal view **21** FSCA 00033041 (ex. *P. maculiventris*), head, mesosoma, metasoma, dorsolateral view **22** FSCA 00033040 (ex. *P. maculiventris*), head, mesosoma, metasoma, dorsal view. Scale bars in millimeters.

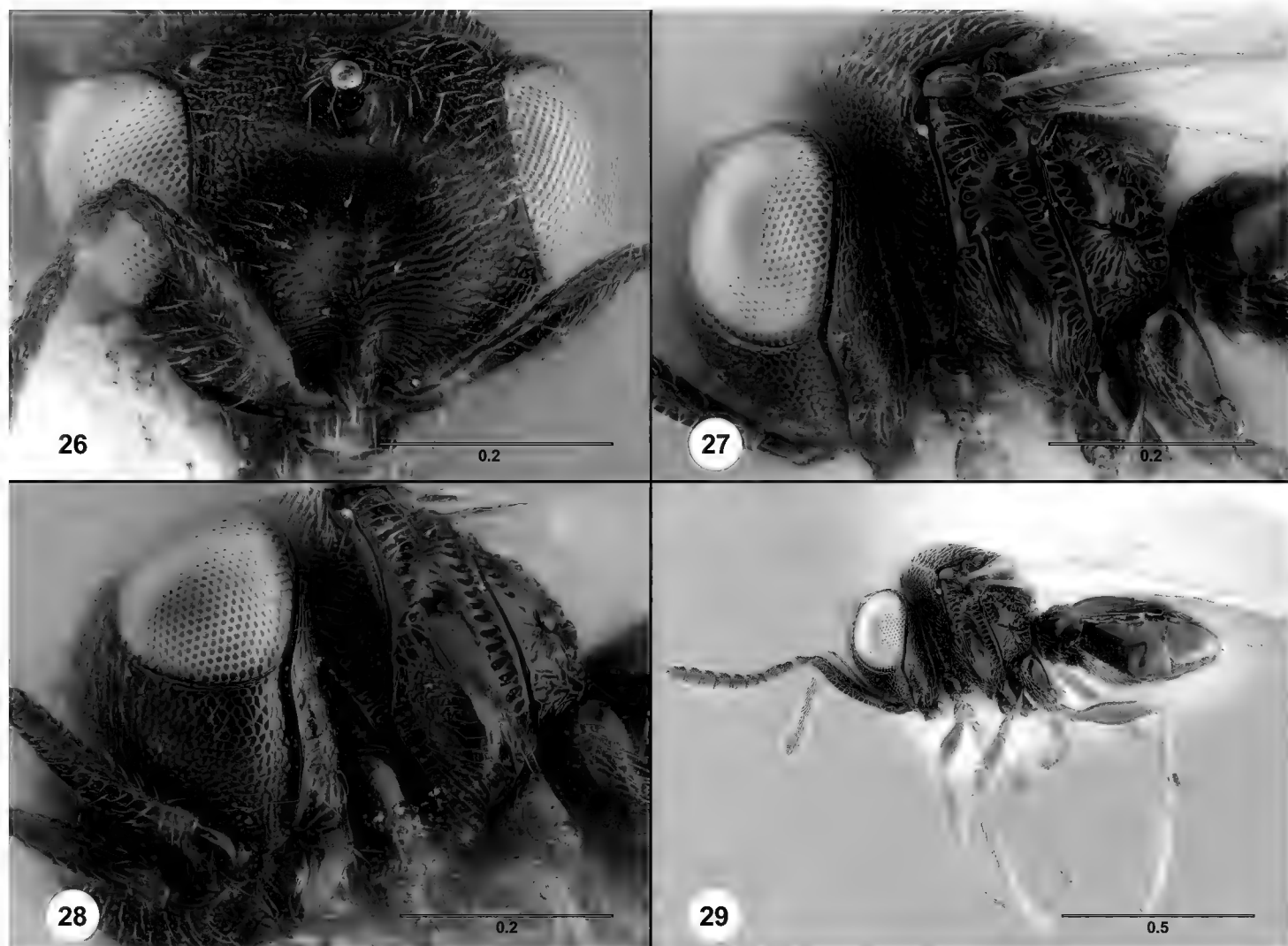


Figures 23–25. *Trissolcus utahensis* (FSCA 00091872, ex. *B. hilaris*) **23** head, anterior view **24** lateral habitus **25** head, mesosoma, metasoma, dorsal view. Scale bars in millimeters.

was the first character listed in the couplet that separates these species in Johnson (1985). Our analysis of specimens in this study lends weight to the reliability of this character.

Color. Most species in *Trissolcus* have a black metasoma. The most notable exception is a Palearctic species, *T. rufiventris* Mayr, in which T2–T7 vary from bright yellow to dark brown. The specimens reared from *B. hilaris* eggs have T2–T7 notably lighter in color than the head and mesosoma (Figs 20, 25), and the body overall is lighter in color than in specimens reared from *P. maculiventris* eggs (compare Fig. 8 to Figs 9–11, Fig. 12 to Figs 13–15).

The most obvious color variation in *T. utahensis* is in the legs. Specimens that parasitized *B. hilaris* eggs have legs that are pale brown to orange distal to the coxae (clades 1, 2; Figs 12, 24). Brightly colored legs were found in *T. utahensis* that emerged from *P. maculiventris* eggs (clade 3, Fig. 29), although the clear majority of specimens reared from *P. maculiventris* eggs in British Columbia had dark brown legs. Interestingly, FSCA 00033239, with pale brown legs, in clade 1 is sister to FSCA 00000320, with dark brown legs. The antennae vary in color in accordance with the legs, although the variation is less pronounced and ranges from medium to dark brown. These data do not indicate that *T. utahensis* exhibits a direct correlation of appendage color with host, size, or lineage.



Figures 26–29. *Trissolcus utahensis* (FSCA 00033042, ex. *P. maculiventris*) **26** head, anterior view **27** head and mesosoma, lateral view **28** head and mesosoma, ventrolateral view **29** lateral habitus. Scale bars in millimeters.

Material Examined. 11 females, FSCA 00091859, 00091872, 00094741–00094749, USA: CA: 33.99105N, 117.33360W, roadside mustard weeds, ex. *Bagrada hilaris* sentinel eggs deployed 6–9.IV.2018, parasitoids emerged 22–23.IV.2018, Coll. F. Ganjisaffar; 1 female, FSCA 00033239, USA: CA: UC Riverside Agricultural Operations, 33.96611N, 117.34230W, squash field with mustard weeds, ex: *Bagrada hilaris* sentinel eggs deployed 12–16-X-2018; parasitoid emerged 27–28-X-2018, Coll. F. Ganjisaffar; 9 females, 2 males, CANADA, BC, Penticton, reared from *Podisus maculiventris*, JUN–AUG-2017, Coll. W. Wong & P. Abram. Egg mass #181: FSCA 00094713–00094715, 00033042–00033043; Egg mass #144: FSCA 00000302; Egg mass #160: FSCA 00094712; Egg mass #92: 00033044–00033045; Egg mass #102; FSCA 00033040–00033041. 1 female, FSCA 00094711, CANADA, BC, Kelowna, reared from *Podisus maculiventris*, 23.V.2017, Coll. W. Wong & P. Abram. Egg mass #171.

Discussion

The reports of this study indicate that at least four species of *Trissolcus* (*T. basalis*, *T. hyalinipennis*, *T. hullensis*, and *T. utahensis*) are actively parasitizing *B. hilaris* eggs

in southern California (Ganjisaffar et al. 2018). Three other scelionids have been reported parasitizing *B. hilaris* eggs in Mexico: *Telenomus podisi* (Ashmead), *Gryon myrmecophilum* (Ashmead), and *Idris elba* Talamas (Felipe-Victoriano et al. 2019, Lomeli-Flores et al. 2019). This suggests that *B. hilaris* eggs may be broadly suitable for Nearctic parasitoids. We conducted surveys in the same locations as Reed et al. (2013) did monthly samplings of *B. hilaris* in 2011, and the fact that we did not find any *B. hilaris* in those areas during our two-year survey, suggests that populations of *B. hilaris* have steadily declined in recent years, and it is likely that parasitoids are part of the cause.

Trissolcus utahensis exhibits a striking degree of variation in *COI* among specimens from only a few localities. An expansion of this analysis with additional samples is certain to expand our understanding of genetic diversity in this species. It is worth noting that specimens FSCA 00094713–00094715 emerged from the same egg mass and were retrieved in different clades (1 and 3), indicating that interbreeding opportunities exist between these maternally definable populations. Future work should include nuclear genes to provide a broader view of population dynamics and genetic diversity in this species.

The systematics of *Trissolcus* is undergoing perpetual improvement as it continues to receive attention for the species that attack the eggs of economically important stink bugs. This study demonstrates how a seemingly routine activity of rearing and identifying specimens can require a multifaceted research endeavor to reach a satisfactory answer while also providing new lines of inquiry. For example, our molecular analysis retrieved *T. colemani* in two clades, one comprised of specimens from East Asia and one from Europe and the Middle East. This study also demonstrates how ongoing parasitoid surveys continue to be productive by providing fresh specimens with host association data. These specimens and data are instrumental for an integrated approach to systematics in which morphological, molecular, and behavioral data are combined to provide robust and holistic species concepts.

Acknowledgements

We thank Shayla Hampel and Colt Bellman for their assistance with bagrada bug colony maintenance and Tim Lewis for his assistance in mapping survey locations and placing and retrieving sentinel egg cards. Brian Hogg and Charlie Pickett developed the sentinel card design used in this study. We also thank Matthew Moore, Cheryl Roberts and Lynn Combee (FDCAS-DPI) for their assistance with generating COI barcodes; and Marie Roche (EBCL) for rearing and identifying specimens of *T. colemani* in France. This project was supported in part by the Florida Department of Agriculture and Consumer Services-Division of Plant Industry, USDA-APHIS Farm Bill: Biological Control of Bagrada Bug, and California Department of Food and Agriculture Specialty Crops Grant Program # SCB16053.

References

Arakelian G (2008) Bagrada bug (*Bagrada hilaris*). Los Angeles County Agricultural Commissioner/ Weights and Measures Department, Arcadia.

Bundy CS, Grasswitz TR, Sutherland C (2012) First report of the invasive stink bug *Bagrada hilaris* (Burmeister) (Heteroptera: Pentatomidae) from New Mexico, with notes on its biology. *Southwestern Entomologist* 37: 411–414. <https://doi.org/10.3958/059.037.0317>

Clement M, Posada D, Crandall KA (2000) TCS: a computer program to estimate gene genealogies. *Molecular Ecology* 9: 1657–1659. <https://doi.org/10.1046/j.1365-294x.2000.01020.x>

Craaud A, Jabbour-Zahab R, Genson G, Craaud C, Couloux A, Kjellberg F, Van Noort S, Rasplus J-Y (2009) Laying the foundations for a new classification of Agaonidae (Hymenoptera: Chalcidoidea), a multilocus phylogenetic approach. *Cladistics* 26: 359–387. <https://doi.org/10.1111/j.1096-0031.2009.00291.x>

Faúndez EI, Luer A, Cuevas ÁG (2017) The establishment of *Bagrada hilaris* (Burmeister, 1835) (Heteroptera: Pentatomidae) in Chile, an avoidable situation? *Arquivos Entomológicos* 17: 239–241.

Faúndez EI, Luer A, Cuevas ÁG, Rider DA, Valdebenito P (2016) First record of the painted bug *Bagrada hilaris* (Burmeister, 1835) (Heteroptera: Pentatomidae) in South America. *Arquivos Entomológicos* 16: 175–179.

Felipe-Victoriano M, Talamas EJ, Sánchez-Peña SR (2019) Scelionidae (Hymenoptera) parasitizing eggs of *Bagrada hilaris* (Hemiptera: Pentatomidae) in Mexico. In: Talamas E (Ed.) Advances in the Systematics of Platygastroidea II. *Journal of Hymenoptera Research* 73: 143–152. <https://doi.org/10.3897/jhr.73.36654>

Folmer O, Black M, Hoeh W, Lutz R, Vrijenhoek R (1994) DNA primers for amplification of mitochondrial cytochrome c oxidase subunit 1 from diverse metazoan invertebrates. *Molecular Marine Biology and Biotechnology* 3: 294–299.

Ganjisaffar F, Talamas EJ, Bon MC, Gonzalez L, Brown BV, Perring TM (2018) *Trissolcus hyalinipennis* Rajmohana & Narendran (Hymenoptera, Scelionidae), a parasitoid of *Bagrada hilaris* (Burmeister) (Hemiptera, Pentatomidae), emerges in North America. *Journal of Hymenoptera Research* 65: 111–130. <https://doi.org/10.3897/jhr.65.25620>

Hernández-Chávez L, Salas-Araiza MD, Martínez-Jaime OA, Flores-Mejía S (2018) First report of *Bagrada hilaris* Burmeister, 1835 (Hemiptera: Pentatomidae) in the state of Guanajuato, Mexico. *Entomological News* 128: 72–74. <https://doi.org/10.3157/021.128.0110>

Howard CW (1907) The Bagrada bug (*Bagrada hilaris*). *Transvaal Agricultural Journal* 5: 168–73.

Huang T, Reed DA, Perring TM, Palumbo JC (2014) Feeding damage by *Bagrada hilaris* (Hemiptera: Pentatomidae) and impact on growth and chlorophyll content of Brassicaceous plant species. *Arthropod-Plant Interactions* 8: 89–100. <https://doi.org/10.1007/s11829-014-9289-0>

Husain MA (1924) Annual report of the entomologist to government, Punjab, Lyallpur for the year ending 30th June 1924. *Punjab Department of Agriculture Reports* 1: 55–90.

Johnson NF (1985) Systematics of New World *Trissolcus* (Hymenoptera: Scelionidae): species related to *T. basalis*. The Canadian Entomologist 117: 431–445. <https://doi.org/10.4039/Ent117431-4>

Kimura M (1980) A simple method for estimating evolutionary rate of base substitutions through comparative studies of nucleotide sequences. Journal of Molecular Evolution 16: 111–120. <https://doi.org/10.1007/BF01731581>

Kumar S, Stecher G, Li M, Knyaz C, Tamura K (2018) MEGA X: Molecular Evolutionary Genetics Analysis across computing platforms. Molecular Biology and Evolution 35: 1547–1549. <https://doi.org/10.1093/molbev/msy096>

Lomeli-Flores JR, Rodríguez-Rodríguez SE, Rodríguez-Levy E, González-Hernández H, Gariepy TD, Talamas EJ (2019) Field studies and molecular forensics identify a new association: *Idris elba* Talamas, sp. nov. parasitizes the eggs of *Bagrada hilaris* (Burmeister). In: Talamas E (Ed.) Advances in the Systematics of Platygastroidea II. Journal of Hymenoptera Research 73: 125–141. <https://doi.org/10.3897/jhr.73.38025>

Mahmood R, Jones WA, Bajwa BE, Rashid K (2015) Egg parasitoids from Pakistan as possible classical biological control agents of the invasive pest *Bagrada hilaris* (Heteroptera: Pentatomidae). Journal of Entomological Science 50: 147–149. <https://doi.org/10.18474/JES14-28.1>

Martel G, Augé M, Talamas E, Roche M, Smith L, Sforza RFH (2019) First laboratory evaluation of *Gryon gonikopalense* (Hymenoptera: Scelionidae), as potential biological control agent of *Bagrada hilaris* (Hemiptera: Pentatomidae). Biological Control 135: 48–56. <https://doi.org/10.1016/j.biocontrol.2019.04.014>

Matsunaga JN (2014) Bagrada bug, *Bagrada hilaris* (Burmeister) (Hemiptera: Pentatomidae). State of Hawaii Department of Agriculture. New pest advisory 14: 1–2. <http://hdoa.hawaii.gov/pi/files/2013/01/Bagrada-hilaris-NPA12-9-14.pdf>

Palumbo JC (2015) Soil-surface-applied insecticides for control of *Bagrada hilaris* (Hemiptera: Pentatomidae) in broccoli, 2014. Arthropod Management Tests 40: 1–2. <https://doi.org/10.1093/amt/tsv203>

Palumbo JC, Natwick ET (2010) The bagrada bug (Hemiptera: Pentatomidae): a new invasive pest of cole crops in Arizona and California. Plant Health Progress 11(1): 1–3. <https://doi.org/10.1094/PHP-2010-0621-01-BR>

Palumbo JC, Perring TM, Millar J, Reed DA (2016) Biology, ecology, and management of an invasive stink bug, *Bagrada hilaris*, in North America. Annual Review of Entomology 61: 453–473. <https://doi.org/10.1146/annurev-ento-010715-023843>

Perring TM, Reed DA, Palumbo JC, Grasswitz T, Bundy CS, Jones WA, Papes M, Royer T (2013) National pest alert-bagrada bug. <https://www.ncipmc.org/projects/pest-alerts1/bagrada-bug-bagrada-hilaris-burmeister/>

Power N, Ganjisaffar F, Perring TM (2020a) Effect of temperature on the survival and developmental rate of immature *Ooencyrtus* sp. (Hymenoptera: Encyrtidae). Journal of Economic Entomology 113(4): 1675–1684. <https://doi.org/10.1093/jee/toaa110>

Power N, Ganjisaffar F, Perring TM (2020b). Evaluation of the physiological host range for the parasitoid *Ooencyrtus mirus*, a potential biocontrol agent of *Bagrada hilaris*. Insects 11(7): e432. <https://doi.org/10.3390/insects11070432>

Rajmohana K (2006) A checklist of the Scelionidae (Hymenoptera: Platygastroidea) of India. Zoos' Print Journal 21: 2506–2513. <https://doi.org/10.11609/JoTT.ZPJ.1570.2506-13>

Ratnasingham S, Hebert PD (2007) BOLD: The Barcode of Life Data System (<http://www.barcodinglife.org>). Molecular Ecology Notes 7: 355–364. <https://doi.org/10.1111/j.1471-8286.2007.01678.x>

Reed DA, Ganjisaffar F, Palumbo JC, Perring TM (2017) Effects of temperatures on immature development and survival of the invasive stink bug *Bagrada hilaris* (Hemiptera: Pentatomidae). Journal of Economic Entomology 110: 2497–2503. <https://doi.org/10.1093/jee/tox289>

Reed DA, Palumbo JC, Perring TM, May C (2013) *Bagrada hilaris* (Burmeister), an invasive stink bug attacking cole crops in the southwestern United States. Journal of Integrated Pest Management 4: 1–7. <https://doi.org/10.1603/IPM13007>

Ronquist F, Teslenko M, van der Mark P, Ayres D, Darling A, Höhna S, Larget B, Liu L, Suchard M, Huelsenbeck J (2012) MrBayes 3.2: efficient Bayesian phylogenetic inference and model choice across a large model space. Systematic Biology 61: 539–542. <https://doi.org/10.1093/sysbio/sys029>

Sabbatini Peverieri G, Talamas E, Bon MC, Marianelli L, Bernardinelli I, Malossini G, Benvenuto L, Roversi PF, Hoelmer K (2018) Two Asian egg parasitoids of *Halyomorpha halys* (Stål) (Hemiptera, Pentatomidae) emerge in northern Italy: *Trissolcus mitsukurii* (Ashmead) and *Trissolcus japonicus* (Ashmead) (Hymenoptera, Scelionidae). Journal of Hymenoptera Research 67: 37–53. <https://doi.org/10.3897/jhr.67.30883>

Sánchez-Peña SR (2014) First record in Mexico of the invasive stink bug *Bagrada hilaris*, on cultivated crucifers in Saltillo. Southwestern Entomologist 39: 375–377. <https://doi.org/10.3958/059.039.0219>

Sforza RFH, Bon MC, Martel G, Agué M, Roche M, Mahmood R, Smith L (2017) 14.2 Initial evaluation of two native egg parasitoids for the control of *Bagrada hilaris*, an invasive stink bug in western USA. Proceedings of the 5th International Symposium on Biological Control of Arthropods, Langkawi, Malaysia, September 11–15, 332 pp.

Sharma SK (1982) On some scelionidae (Proctotrupoidea: Hymenoptera) from India. Records of the Zoological Survey of India 80: 319–342.

Simon C, Buckley TR, Frati F, Stewart JB, Beckenbach AT (2006) Incorporating molecular evolution into phylogenetic analysis, and a new compilation of conserved polymerase chain reaction primers for animal mitochondrial DNA. Annual Review of Ecology, Evolution and Systematics 37: 545–579. <https://doi.org/10.1146/annurev.ecolsys.37.091305.110018>

Srivathsan A, Meier R (2012) On the inappropriate use of Kimura-2-parameter (K2P) divergences in the DNA-barcoding literature. Cladistics 28: 190–194. <https://doi.org/10.1111/j.1096-0031.2011.00370.x>

Talamas EJ, Johnson NF, Buffington M (2015) Key to Nearctic species of *Trissolcus* Ashmead (Hymenoptera, Scelionidae), natural enemies of native and invasive stink bugs (Hemiptera, Pentatomidae). Journal of Hymenoptera Research 43: 45–110. <https://doi.org/10.3897/jhr.43.8560>

Talamas EJ, Buffington ML, Hoelmer K (2017) Revision of Palearctic *Trissolcus* Ashmead (Hymenoptera, Scelionidae). In: Talamas EJ, Buffington ML (Eds) Advances in the Systematics of Platygastroidea. Journal of Hymenoptera Research 56: 3–185. <https://doi.org/10.3897/jhr.56.10158>

Talamas EJ, Bon M-C, Hoelmer KA, Buffington ML (2019) Molecular phylogeny of *Trissolcus* wasps (Hymenoptera, Scelionidae) associated with *Halyomorpha halys* (Hemiptera, Pentatomidae). In: Talamas E (Ed.) Advances in the Systematics of Platygastroidea II. Journal of Hymenoptera Research 73: 201–217. <https://doi.org/10.3897/jhr.73.39563>

Thompson JD, Higgins DG, Gibson TJ (1994) CLUSTAL W: Improving the sensitivity of progressive multiple sequence alignment through sequence weighting, position specific gap penalties and weight matrix choice. Nucleic Acids Research 22: 4673–4680. <https://doi.org/10.1093/nar/22.22.4673>

Torres-Acosta RI, Sánchez-Peña SR (2016) Geographical distribution of *Bagrada hilaris* (Hemiptera: Pentatomidae) in Mexico. Journal of Entomological Science 51: 165–167. <https://doi.org/10.18474/JES15-41.1>

Tortorici F, Talamas EJ, Moraglio ST, Pansa MG, Asadi-Farfar M, Tavella L, Caleca V (2019) A morphological, biological and molecular approach reveals four cryptic species of *Trissolcus* Ashmead (Hymenoptera, Scelionidae), egg parasitoids of Pentatomidae (Hemiptera). In: Talamas E (Ed.) Advances in the Systematics of Platygastroidea II. Journal of Hymenoptera Research 73: 153–200. <https://doi.org/10.3897/jhr.73.39052>

Triapitsyn S, Andreason S, Power N, Ganjisaffar F, Fusu L, Dominguez C, Perring T (2020) Two new species of *Ooencyrtus* (Hymenoptera, Encyrtidae), egg parasitoids of the bagrada bug *Bagrada hilaris* (Hemiptera, Pentatomidae), with taxonomic notes on *Ooencyrtus telenomicida*. Journal of Hymenoptera Research 76: 57–98. <https://doi.org/10.3897/jhr.76.48004>

Vitanza S (2012) Issues in agriculture. Texas A&M AgriLife Extension Newsletter 38: 1–8.